

A Study of Quasar Radio Emission from the VLA FIRST Survey

Yogesh Wadadekar,¹ and Ajit Kembhavi²

Inter University Centre for Astronomy and Astrophysics, Post Bag 4, Ganeshkhind, Pune 411007,
India

ABSTRACT

Using the most recent (1998) version of the VLA FIRST survey radio catalog, we have searched for radio emission from 1704 quasars taken from the most recent (1993) version of the Hewitt and Burbidge quasar catalog. These quasars lie in the ~ 5000 square degrees of sky already covered by the VLA FIRST survey. Our work has resulted in positive detection of radio emission from 389 quasars of which 69 quasars have been detected for the first time at radio wavelengths. We find no evidence of correlation between optical and radio luminosities for optically selected quasars. We find indications of a bimodal distribution of radio luminosity, even at a low flux limit of 1 mJy. We show that radio luminosity is a good discriminant between radio loud and radio quiet quasar populations, and that it may be inappropriate to make such a division on the basis of the radio to optical luminosity ratio. We discuss the dependence of the radio loud fraction on optical luminosity and redshift.

Subject headings: quasars: general– methods: statistical– catalogs– surveys

1. INTRODUCTION

It has been well known for some time that only about 10% of quasars are radio loud, with radio luminosity comparable to optical luminosity. This is surprising, because over a very wide wavelength range from $100 \mu\text{m}$ through X-ray wavelengths, the properties of radio loud and radio quiet quasars are very similar. The presence or absence of a radio component may be a pointer to different physical processes occurring in the two types of quasar, but it is not yet clear as to what these processes are.

The relationship between quasar radio and optical emission was initially studied using radio selected objects, which generally had high radio luminosities because the early radio surveys had relatively high limiting radio fluxes. Sandage (1965) showed that not all quasars are powerful

¹yogesh@iucaa.ernet.in

²akk@iucaa.ernet.in

combining a large sky coverage with a low flux limit of 1 mJy at 20 cm. This ongoing survey, when completed will cover 10,000 square degrees around the North Galactic Cap, the same area of the sky to be surveyed by the Sloan Digital Sky Survey (SDSS; <http://www.sdss.org/>). To date, data for approximately one half of the eventual sky coverage have been released.

FIRST allows us to address the issue of quasar bimodal radio luminosity distribution in two different but complementary ways. Firstly, optical identifications of FIRST sources using large optical surveys such as the Palomar Observatory Sky Survey (POSS) provide a large database of quasar candidates, whose true nature can then be verified spectroscopically. Several such efforts (eg. Gregg *et al.* 1996; Becker *et al.* 1997) are currently underway. Secondly, the large area covered by the FIRST survey allows us to look for radio emission from a significant fraction of already known quasars and correlate their radio properties with other observables. In the present paper, we have used this approach to determine the radio properties of quasars from the catalog of Hewitt & Burbidge (1993, hereafter HB93).

Such an approach has also been taken, though with a different radio survey and quasar catalog, by Bischof and Becker (1997, hereafter BB97) who compared positions of radio sources from the NVSS radio survey (Condon *et al.* 1998), with the positions of 4079 quasars from the Veron catalog (Veron-Cetty and Veron 1991). They detected radio emission from 799 quasars, of which 168 were new radio detections.

The FIRST survey has better sensitivity and resolution than the NVSS, but covers a smaller area. There is a small area of overlap between NVSS and FIRST. The FIRST survey, which is being carried out with the VLA in its B-configuration, has excellent astrometric accuracy of $\sim 1''$ (90% error circle) and a 5 sigma sensitivity of ~ 1 mJy. This compares favorably with the D-array NVSS, which has a beam size of 45 arcsec and a 5 sigma sensitivity of ~ 2.4 mJy. FIRST has a smaller beam size than NVSS, and so it is expected to have better sensitivity to point sources. We look for radio emission from the 1704 quasars from HB93 ($\sim 23\%$ of the quasars listed therein) which lie in the area covered by the FIRST survey. This set of quasars is not statistically complete in any sense. Wherever appropriate, we distinguish between radio selected quasars and those selected by other means.

2. RADIO/OPTICAL COMPARISONS

We compare the positions of quasars in HB93 to the positions of radio sources in the FIRST radio source catalog (February 4, 1998 version available at <http://sundog.stsci.edu/>), and calculate the angular separation between each quasar and each FIRST source. About 4% of sources in the FIRST catalog have been tagged as possible sidelobes of bright sources. Of these, $<10\%$ are real sources and considerably less than 1% of the unflagged sources in the catalog are sidelobes (White *et al.* 1997). We have excluded these flagged sidelobe sources from our cross correlation. We are then left with a total of 421,447 unflagged sources in the northern and southern strips, covering a

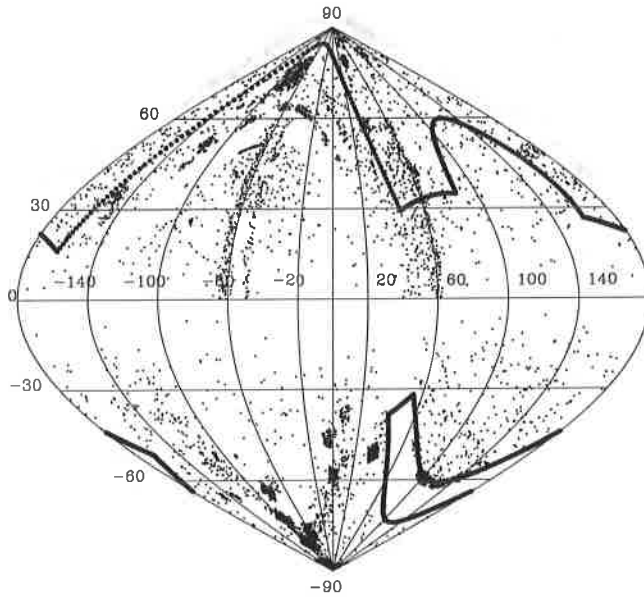


Fig. 1.— The approximate boundaries, in galactic coordinates, of the areas covered by the FIRST survey are indicated by bold points. The northern and southern strips are separately shown. The dots indicate quasars from the Hewitt and Burbidge (1993) catalog.

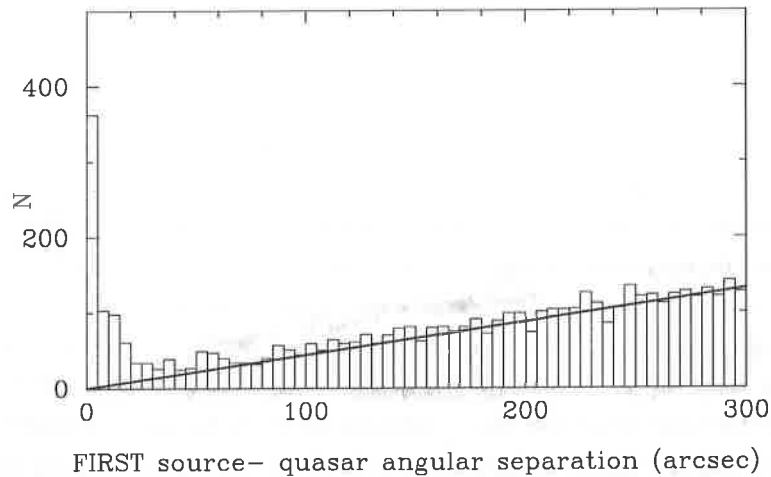


Fig. 2.— A histogram of the angular separation between the Hewitt and Burbidge (1993) quasars and the corresponding FIRST source. The straight line is the number of chance matches expected, for a search area of radius shown on the X-axis, if the FIRST sources were randomly distributed in the sky.

in Table 2 (Note: Only a sample partial page is provided here. The full table is available in the electronic version of this paper). Detections in the radio reported after the quasar catalog was published (mostly in BB97) are mentioned in the last column. Those quasars which do not have the letter R in the selection technique code and do not have a recent radio detection mentioned in the last column may be considered to be the new detections. There are 69 such quasars in Table 2. The last eight entries are the additional list of matches obtained using a correlation with the USNO-A2.0 catalog. These 8 matches were obtained using an indirect comparison technique, and have *not* been used in the statistical correlations reported in subsequent sections.

2.1. 1343+266: not a gravitationally lensed quasar?

This is a close pair of quasars with identical redshift, similar spectra and separated by only ~ 10 arcsec. Detailed spectroscopic observations have shown qualitative (eg. presence of certain lines) as well as quantitative (eg. ratio of line strengths) *differences* between the two quasars, strengthening the claim that this is *not* a gravitationally lensed pair, but a physically associated pair of quasars, possibly residing in a cluster of galaxies at $z = 2.03$ (Crampton *et al.* 1988; Crofts *et al.* 1994). The optical luminosities are comparable, with 1343+266B having a luminosity higher by about 5% than 1343+266A. We find radio emission from only one of the quasars: 1343+266B has a flux of 8.9 mJy. The separation between the gravitationally lensed quasar and the FIRST source is 2.18 arcsecond, which is consistent with an error of $\sim 1''$ each in the quasar optical position and the FIRST radio position. There is no radio emission associated with 1343+266A at the FIRST flux limit of 1 mJy, because the FIRST source associated with 1343+266B is 7.4 arcsec away, too far to be associated with 1343+266A, considering the extremely accurate astrometry done for this well studied pair of quasars. There is no other FIRST source associated with 1343+266A. This implies that the radio luminosity of 1343+266B is at least 8.9 times higher than that of 1343+266A, in sharp contrast to only 5% difference in their optical luminosity. Such radio detection is strong evidence that the pair is *not* gravitationally lensed.

3. RADIO AND OPTICAL PROPERTIES

3.1. Bivariate luminosity functions

The number of quasars with optical luminosity in the range $(L_{\text{op}}, L_{\text{op}} + dL_{\text{op}})$, radio luminosity in the range $(L_{\text{r}}, L_{\text{r}} + dL_{\text{r}})$ and redshift in the range $(z, z + dz)$ is in general given by $\Phi(L_{\text{op}}, L_{\text{r}}, z)dL_{\text{op}}dL_{\text{r}}dv(z)$, where the *luminosity function* $\Phi(L_{\text{op}}, L_{\text{r}}, z)$ is the comoving number density of quasars for unit ranges of the respective luminosities, and $dv(z)$ is a comoving volume element at z . If the radio and optical luminosities are independently distributed, it is possible to separate the luminosity function as

of magnitude, and the redshift goes upto ~ 3.6 . All three kinds of quasar are distributed over much of these wide ranges.

3.2. Distribution of radio luminosity

The radio-selected quasars (RSQ) in our sample have all been discovered in radio surveys with flux limits much higher than the 1 mJy limit of the FIRST survey. For a given redshift, these quasars will have much higher radio luminosity than most of the non-radio selected component of our population. The radio luminosity distribution of the RSQ is consequently not representative of the distribution for the overall quasar population. We shall therefore omit the RSQ from the following considerations, except where they are needed in some specific context.

We have shown in Figure 4 a plot of the 5 GHz radio luminosity against redshift for non-radio selected quasars. The OSQD are shown as unfilled circles, while the OSQU are shown as dots, and form the almost continuous lower envelope which indicates the radio luminosity corresponding to a radio flux of 1 mJy over the redshift range. In Figure 5 is shown a plot of the 5 GHz radio luminosity against the absolute blue magnitude for the non-radio selected quasars. In this figure too, radio detections are shown as open circles, and the radio upper limits as dots. There appears to be a correlation between the logarithm of the radio luminosity and absolute magnitude, in spite of the large scatter in radio luminosity for a given absolute magnitude. The linear correlation coefficient for the 135 radio detections alone is 0.22, which is significant at the > 99.9 percent confidence level. However, it is seen from Figure 3 and Figure 4 that mean radio as well as optical luminosity increase with redshift, which is due to the existence of a limiting radio flux and apparent magnitude in the surveys in which quasars are discovered. A situation can arise in which an observed correlation between radio luminosity and absolute magnitude is mainly due to the dependence of each luminosity on the redshift z . It is important to see if the correlation remains significant when such an effect of the redshift on the observed correlation is taken into account. This can be done by evaluating a *partial linear correlation coefficient* as follows (Havilcek & Crain 1988; Kembhavi & Narlikar 1999).

Let $r_{L_r, M}$, $r_{L_r, z}$ and $r_{M, z}$ be the correlation coefficients between the pairs $\log L_r$ and M , $\log L_r$ and z , and M and z respectively. The partial linear correlation coefficient is then defined by

$$r_{L_r, M; z} = \frac{r_{L_r, M}^2 - r_{L_r, z} r_{M, z}}{\sqrt{1 - r_{L_r, z}^2} \sqrt{1 - r_{M, z}^2}} \quad (5)$$

The partial correlation coefficient has the same statistical distribution as the ordinary correlation coefficient and therefore the same tests of significance can be applied to it. A statistically significant value for it means that the luminosities are correlated at that level of significance even after accounting for their individual dependence on the redshift.

For our sample of 135 radio detections, the partial linear correlation coefficient is 0.09, which

is significant only at the 72 percent confidence level. The observed correlation between the radio luminosity and absolute magnitude thus appears to be largely induced by the effect of the large range in redshift over which the sample is observed. The lack of correlation found here is consistent with the results of Miller, Peacock and Mead (1990, hereafter MPM90) and Hooper *et al.* (1995).

MPM90 have observed a sample of optically selected quasars, with redshift in the range $1.8 < z < 2.5$, with the VLA to a limiting sensitivity of ~ 1 mJy at 5 GHz. They detected nine quasars out of a sample of 44; these objects are shown in Figure 5 as filled squares. The radio upper limits of MPM90 occupy the same range as our upper limits shown in the figure, and are not separately indicated. MPM90 have commented at length on the luminosity gap found between their radio detections and upper limits. They concluded that the gap was indicative of a bimodality in the distribution of radio luminosity, which divides quasars into a radio loud population, with radio luminosity $> 10^{25} \text{ W Hz}^{-1} \text{ str}^{-1}$, and a radio quiet population with luminosity $< 10^{24} \text{ W Hz}^{-1} \text{ str}^{-1}$. The radio loud quasars were taken to be highly luminous representatives of the population of radio galaxies, and the radio quiet population was taken to be like Seyfert galaxies. The conspicuous gap between radio detections and upper limits is absent in our data. It is seen in Figure 5 that the region $\sim 10^{32} \lesssim L_r(5 \text{ GHz}) \lesssim 10^{33} \text{ erg sec}^{-1} \text{ Hz}^{-1}$ (which corresponds to the gap found by MPM90 for our units and constants) is occupied by many quasars. Only seven of these are in the redshift range of the MPM90 sample, which probably explains why they did not find any quasars in the gap: our sample is about 30 times larger, and even then we find only a small number in the range.

In Figure 6 we show the distribution of the log of radio luminosity for the RSQ, the OSQD and the OSQU. The mean value for each is indicated by an arrow. The radio luminosity of the OSQD has a mean value of $10^{32.24} \text{ erg sec}^{-1} \text{ Hz}^{-1}$, which is approximately 1.5 orders of magnitude fainter than the mean luminosity of the RSQ, because the latter were selected in high flux limit surveys. The RSQ have a median radio flux of ~ 400 mJy, while there are only three OSQD with radio flux ≥ 100 mJy. The radio luminosity upper limits of the OSQU are well mixed with the fainter half of the luminosity distribution of the OSQD. The rather sharp cutoff in the luminosity upper limit distribution of the OSQU is due to the flattening in the 1 mJy luminosity envelope in Figure 4 at high redshifts. The upper limits peak at a luminosity which is approximately half a decade lower than the peak in the luminosity distribution of the OSQD. The mean value for the OSQU is $10^{31.55} \text{ erg sec}^{-1} \text{ Hz}^{-1}$. A Kolmogorov-Smirnov test on the distribution of radio luminosity of the OSQD and OSQU shows that they are drawn from different distributions with a significance of 99.9 percent. This is consistent with a bimodal distribution amongst the radio detections and upper limits. If the radio luminosity distribution is indeed bimodal, the present radio upper limits, when observed to a limiting flux significantly less than 1 mJy, would be found to have radio luminosities considerably lesser than the present set of detections.

3.3. Distribution of radio-to-optical luminosity ratio R

The ratio R is defined using rest frame monochromatic radio and optical luminosities at some fiducial rest frame wavelengths. In the following we will choose these to be at 5 GHz and 2500 Å in the radio and optical case respectively. With our choice of spectral indices $\alpha_r = \alpha_{op} = 0.5$, $\log R$ is given in terms of observed flux densities at observed wavelengths at 5 GHz and 2500 Å by

$$\log R = \log F_r(5 \text{ GHz}) - \log F_{op}(2500 \text{ Å}). \quad (6)$$

Figure 7 shows the variation of R with redshift. There is considerable overlap for $R \lesssim 3$ between the radio detections and upper limits, but there are only detections at the highest values of R . There is only one upper limit with $R > 3$. At each redshift, there is a maximum to the R upper limits, and this increases slowly with redshift, so that an envelope is seen. For an upper limit to be found above the envelope, it would be necessary to have quasars at fainter optical magnitudes than are presently to be found in the HB catalogue. In the case of the detections, the maximum value $R_{\max}(z) = L_{r,\max}(z)/L_{op,\min}(z)$ decreases with redshift. This occurs because the increase in $L_{r,\max}(z)$ with redshift is slower than the increase in $L_{op,\min}(z)$ with redshift, as can be seen from Figure 3 and Figure 4. Similarly, the minimum value of R for the detections, $R^{\min}(z) = L_{r,\min}(z)/L_{op,\max}(z)$, increases with redshift, because $L_{op,\max}(z)$ increases slower than $L_{r,\min}(z)$.

Figure 8 shows a histogram of $\log R$ for radio detections (solid line) and radio upper limits (dashed line). For comparison, the distribution of R for the radio selected quasars is shown as a dotted line. An important question here is whether the distribution of R is bimodal. The number of radio detections is not large enough to provide information about the distribution of R over its wide range. However, as mentioned above, there is considerable overlap in the distributions of the detections and upper limits in the region $0 \leq R \leq 3$. It is therefore possible, in principle, to use statistical techniques from the field of survival analysis (see e.g. Feigelson and Nelson 1985) to determine the underlying distribution for a mixed sample of detections and upper limits. If this joint distribution, and the overall distribution of detections have distinct maxima, then one could say that the distribution of R amongst all quasars is bimodal.

The appropriate technique to derive the joint distribution would be the Kaplan-Meier estimator included as part of the ASURV package (LaValley, Isobe & Feigelson, 1992). One of the requirements of this estimator is that the probability that an object is censored (ie, it has an upper limit), is independent of the value of the censored variable. If such *random censoring* applies to our sample, then the shape of the observed distribution of R for the detections and upper limits should be the same, in the region of overlap $0 \leq R \leq 3$. A Kolmogorov-Smirnov test shows that the two distributions may be considered to be drawn from the same population at only the ~ 20 percent level of significance. Due to the low level of significance it is not possible to use the Kaplan-Meier estimator, or another similar to it, to obtain a joint distribution. A radio survey

with a lower limiting flux than FIRST would be needed to convert the upper limits to detections and to constrain the distribution of R at its lower end. Additional quasars with higher R values can be found by increasing the area covered by the FIRST survey.

We have mentioned in subsection 3.1 that the separation of the bivariate luminosity function as in Equation 2 is most useful if R is independent of the optical luminosity. Moreover, such a separation implies that the mean radio luminosity must increase with the optical luminosity. Such a correlation between the luminosities is not seen in Figure 5, and as discussed in subsection 3.2, L_r appears to be distributed independently of L_{op} (ie, absolute magnitude). This requires that the distribution of R depends on L_{op} and separation as in Equation 2 is not possible. Separation of the bivariate function as in Equation 1 therefore appears to be the preferred alternative.

4. Radio-loud Fraction

As mentioned in the introduction, the boundary between radio loud and radio quiet quasars can be defined either (1) in terms of a characteristic value of the radio to optical luminosity ratio R , say $R = 1$, or (2) in terms of a characteristic radio luminosity. These two criteria are related to the two ways in which the bivariate luminosity function can be split up between the optical and radio parts as discussed in subsection 3.1. We have found no correlation between the radio and optical luminosities, which implies that a separation involving R , as in Equation 2 is not consistent with the data. The distribution of R therefore must be luminosity dependent, and using a single value of R for separation between radio loud and quiet populations is not appropriate. In this situation, we prefer to adopt the criterion for radio loudness which uses radio luminosity as the discriminant as in MPM90.

The dividing radio luminosity chosen by MPM90, in our units, is $10^{33.1} \text{ erg sec}^{-1} \text{ Hz}^{-1}$. This choice was made on the basis of a clear separation between radio detections and upper limits observed by them, which we do not find, as explained in subsection 3.2. We have shown the MPM90 division with a dashed line in Figure 5. It is seen that there is a region below this line with a number of FIRST survey radio detections, but no upper limits. It is therefore possible for us to reduce the dividing luminosity to a level of $10^{32.5} \text{ erg sec}^{-1} \text{ Hz}^{-1}$, which is indicated by a solid line in the figure. We define as radio loud all quasars with $L_r(5 \text{ GHz}) > 10^{32.5} \text{ erg sec}^{-1} \text{ Hz}^{-1}$, and as radio quiet all quasars below this limit, even though they may have detectable radio emission. The radio loud objects tend to have bright absolute magnitudes, while a dominating fraction of the radio quiet detections have $M_B > -25$. The faintest of the latter objects could perhaps be active galaxies like Seyferts, which in the local neighborhood are known to have lower radio luminosities than radio galaxies. The radio loud quasars can be considered to be luminous counterparts of the radio galaxies, as in the unification model (Barthel 1989). If the radio loud and quiet classes indeed represent such a physical division, then the host galaxies of the former would perhaps be elliptical, as is the case with radio galaxies, while the hosts of the quiet objects would be disk galaxies like the Seyferts. Deep optical and near-IR imaging of different types of quasars would

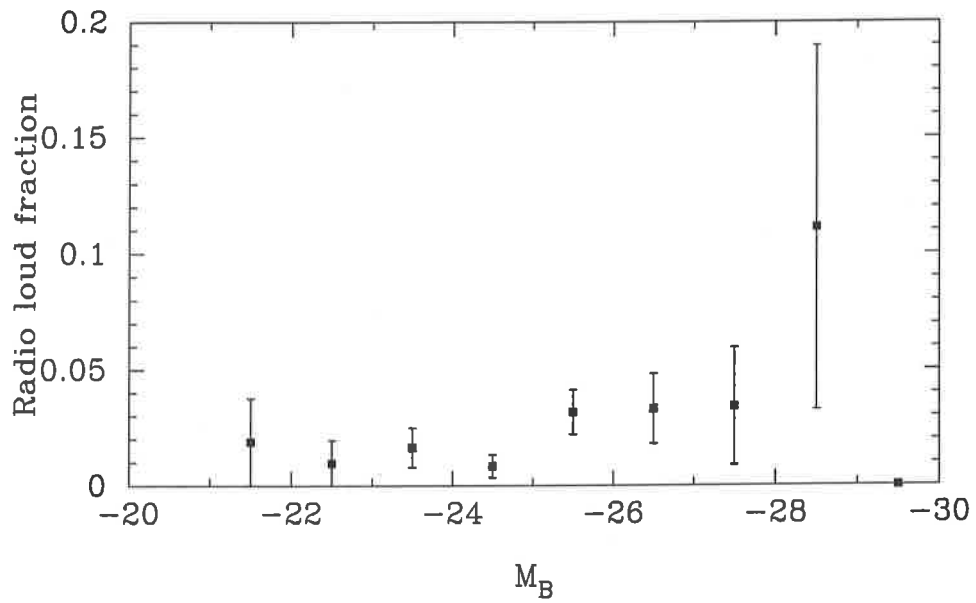


Fig. 9.— Radio loud fraction as a function of absolute magnitude. The error bar shown is the standard deviation for a random binomial distribution in the radio detection fraction.

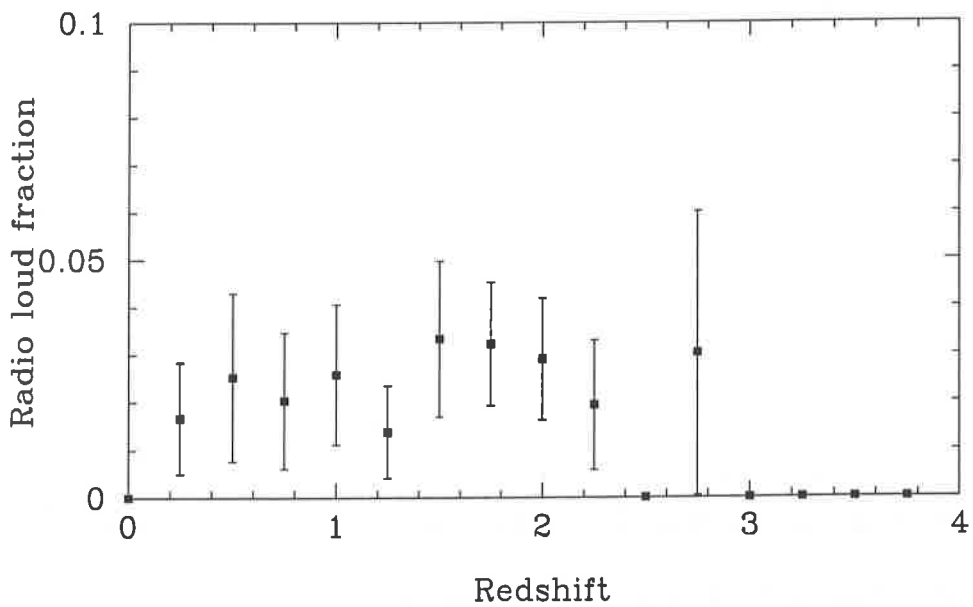


Fig. 10.— Radio loud fraction of quasars as a function of redshift. The error bars are obtained as in Figure 9

- Condon, J. J., Odell, S. L., Puschell, J. J., Stein, W. A. 1981, ApJ, 246, 624
- Condon, J. J., Cotton, W. D., Greisen, E. W., Yin, Q. F., Perley, R. A., Taylor, G. B. & Broderick, J. J. 1998, AJ, 115, 1693
- Crotts, A. P. S., Bechtold, J, Fang, Y. & Duncan, R. C. 1994, ApJ, 437, L79
- Feigelson, E. D. & Nelson, P. I. 1985, ApJ, 293, 192
- Gregg, M. D. Becker, R. H., White, R. L., Helfand, D. J., McMahon, R. G. & Hook, I. M. 1996, AJ, 112, 407
- Havilcek, L. L. & Crain, R. D. 1988, Practical statistics for the physical sciences (Washington DC: American Chemical Society)
- Hewitt A. & Burbidge G. 1993, ApJS, 87, 451
- Hooper, E. J., Impey, C. D., Foltz, C. B. & Hewett, P. C. 1995, ApJ, 445, 62
- Hooper, E. J., Impey, C. D., Foltz, C. B. & Hewett, P. C. 1996, ApJ, 473, 746
- Kellermann, K. I., Sramek, R., Schmidt, M., Shaffer, D. B., & Green, R. 1989, AJ, 98, 1195
- Kellermann, K. I., Sramek, R. A., Schmidt, M., Green, R. F., & Shaffer, D. B. 1994, AJ, 108, 1163
- Kembhavi, A. & Narlikar, J. 1999, Quasars and Active Galactic Nuclei: an Introduction (Cambridge: Cambridge Univ. Press)
- Kukula, M. J., Dunlop, J. S., Hughes, D. H. & Rawlings, S. 1998, MNRAS, 297, 366
- LaValley, M., Isobe, T. & Feigelson, E. 1992, A.S.P. Conference Series, Vol. 25, 245
- Marshall, H.L. 1987, ApJ, 316, 84
- Miller, L., Peacock, J. A., & Mead, A.R.G. 1990, MNRAS, 244, 207
- Monet, D., Bird, A., Canzian, B., Harris, H., Reid, N., Rhodes, A., Sell, S., Ables, H., Dahn, C., Guetter, H., Henden, A., Leggett, S., Levison, H., Luginbuhl, C., Martini, J., Monet, A., Pier, J., Riepe, B., Stone, R., Vrba, F., Walker, R. 1996, USNO-A2.0, (Washington DC: U.S. Naval Observatory)
- Peacock, J. A., Miller, L. & Longair, M. S. 1986, MNRAS, 218, 265
- Sramek, R.A. & Weedman, D.W. 1980, ApJ, 238, 435
- Sandage A. 1965, ApJ, 141, 1560
- Stocke, J. T., Morris, S. L., Weymann, R. J. & Foltz, C. B. 1992, ApJ, 396, 487
- Terlevich, R., Tenorio-Tagle, G., Franco, J. & Melnick, J. 1992, MNRAS, 255, 713
- Veron-Cetty, M.P., & Veron, P. 1991, ESO Scientific Report 10
- Visnovsky, K. L. *et al.* 1992, ApJ, 391, 560
- White, R. L., Becker, R. H., Helfand, D. J., & Gregg, M. D. 1997, ApJ, 475, 479

Table 2. FIRST detections of quasars

IAU Designation	Selection ^a Technique	m_{pg}	1.4 GHz Peak Radio Flux(mJy)	z	Separation (arcsec)	Alternative designation	Recent radio detection
0002-018	O	18.7	62.26	1.71	1.2		
0003-003	R	19.35	3111.27	1.03	0.6	3CR 2	
0004+006	O	17.8	1.55	0.32	1.3		
0009-018	O	18.4	1.61	1.07	2.2	UM 212	
0012-002	O	17.	1.45	1.55	5.0	UM 221	
0012-004	O	18.6	12.67	1.70	0.7		
0013-005	R	20.8	1050.26	1.57	1.6	PKS	
0019+003	O	18.6	1.72	0.31	0.5	A	
0020-020	O	18.4	8.31	0.69	0.4		
0021-010	O	18.2	1.17	0.76	0.7		
0024+003	O	18.0	3.50	1.22	1.7		
0029-018	O	18.7	13.54	2.38	0.3		
0038-020	RX	18.5	593.72	1.17	8.0	PKS	
0038-019	RX	16.86	272.43	1.67	8.4	PKS	
0038-019	RX	16.86	441.62	1.67	8.4	PKS	
0040+005	O	18.	1.09	2.00	2.0	UM 269	
0043+008	OXR	17.	3.04	2.14	1.0	UM 275	
0045-013	O	18.	1.61	2.53	1.3	UM 278	
0045-000	CR	19.4	89.40	1.53	1.4	PKS	
0048+004	O	18.2	13.70	1.18	1.1		
0052-002	O	17.7	3.08	0.64	1.1		
0054-006	R	19.1	114.74	2.77	0.2	PKS	
0056-001	CXR	17.02	2324.98	0.71	0.5	PHL 923	
0059-021	O	18.0	2.37	1.32	0.7		
0100+004	O	19.0	31.65	1.43	4.7		
0101-025	R	19.1	259.45	2.05	3.6	PKS	
0103-021	R	19.84	613.74	2.20	1.4	PKS	
0105-008	R	17.5	883.60	0.31	1.0	PKS	
0107-025	C	18.2	90.65	0.95	2.3	QSO 10	
0112-017	RX	17.41	1025.07	1.36	0.3	PKS	
0122-005	O	18.6	334.34	2.28	1.4	UM 320	
0122-003	R	16.70	1481.35	1.07	0.5	PKS	

Note. — This is a sample partial page. The full table is available in the electronic edition of this paper.

^aSelection Technique O:Objective Prism R: Radio C: UV-Excess X: X-Ray U: Selection technique not mentioned.